Effect of Hybridization on Structure and Bonding of Cluster Compounds Possessing a Square-Pyramidal $Fe_3(CO)_9E_2$ Core (E = Element of Group 15 or 16)

Jeffrey R. Eveland,[†] Jean-Yves Saillard,*[,‡] and Kenton H. Whitmire*[,†]

Department of Chemistry, Rice University, 6100 Main Street, Houston, Texas 77005-1892, and LCSIM-URA 1495, Université de Rennes I, 35042 Rennes Cedex, France

Received March 6, 1996[⊗]

The pyrolysis of $[NEt_4]_2[Bi_4Fe_4(CO)_{13}]$ in MeCN cleanly produces the square-pyramidal cluster $[NEt_4]_2[Fe_3(CO)_9Bi_2]$. An X-ray crystallographic study was carried out on this compound at 223 K (orthorhombic space group $P2_12_12_1$ (No. 19) with $a = 7.280(1)$ Å, $b = 20.642(4)$ Å, $c = 22.365(4)$ Å, $V = 3360.9(10)$ Å^3, and $Z = 4$) showing it to belong to the square-pyramidal class of 50 electron E_2M_3 clusters. When the E atom bears a substituent, the E···E distances are shorter, and the $M_{basal}-E-M_{basal}$ angles are larger than when a lone pair of electrons resides on E. It has become fashionable to attribute such changes in bond parameters to the formation of E−E bonding, but rehybridization of the main group element could also explain this phenomenon. In order to shed light on this fundamental aspect of bonding in E−M clusters, a detailed extended Hückel molecular orbital analysis was undertaken. It appears that weak E−E bonding may be present in some cases but that this is not the dominant effect.

Introduction

Considerable interest has focused recently on compounds that combine main group elements (E) and transition metals (M) in a core framework.[1] New and often surprising structures and bonding situations are continually discovered in these systems. These results show that E serve as important constituents of the cluster frameworks, playing a key role in determining structure and reactivity patterns. An important feature for the heaviest E elements has been their ability to adopt "hypervalent" bonding modes. These extra bonding interactions are obtained at the expense of other E−M, E-ligand, or M-ligand bonding. A system where such secondary interactions may be important is that in which the clusters contain an E_2M_3 core. Examples where the E−E distance is short enough to suggest a significant bonding interaction include $Te_2Fe_3(CO)_9L$,[2] $[Fe_2(CO)_6Bi_2\{\mu\text{-}Co(CO)_4\}]^-$,[3] and $E_2\{W(CO)_5\}_3$ (E = As, Sb, Bi).[4] None of these compounds requires an E−E interaction by classical electron-counting formalisms, but the distances suggest partial bonding for $Te_2Fe_3(CO)_9L$, a single bond for $[Fe_2(CO)_6Bi_2\{\mu\text{-}Co(CO)_4\}]^-$, and multiple bonding in the case of the $E_2\{W(CO)_5\}_3$ compounds. Similar but weaker interactions may be seen in comparing square-pyramidal E_2M_3 clusters with and without substituents at E.[5−20] Selected compounds are provided in Table 1 while a more exhaustive list is provided in the supplementary material.

The compounds given in Table 1 are all isoelectronic, electron-precise, square-pyramidal compounds in which the E atoms occupy *trans*, basal positions. Due to the mixed E−M nature, the cluster core is somewhat distorted from the ideal square-pyramidal geometry. In particular, the M_2E_2 "square" is slightly puckered with bond angles at E and at M differing significantly from 90°. These distortions are related to the rather short E···E nonbonding distances (see Table 1). It is noteworthy that the Fe−E−Fe angle (α) is smaller when E is a bare atom (α ∼ 95−98°) and larger when E is bearing an external substituent (α ∼ 100−102°). This trend has been interpreted as resulting from the presence of a lone pair on the former group and its absence on the latter.[14] Indeed it is well-known that the presence of a lone pair on an sp^3-hybridized atom favors

[†] Rice University.
[‡] Université de Rennes I.
[⊗] Abstract published in *Advance ACS Abstracts,* January 1, 1997.

(1) For recent reviews, see: (a) Scheer, M.; Herrmann, E. *Z. Chem.* **1990**, *30*, 41. (b) Whitmire, K. H. *J. Coord. Chem.* **1988**, *B17*, 95. (c) Norman, N. C. *Chem. Soc. Rev.* **1988**, *17*, 269. (d) Compton, N. A.; Errington, J.; Norman, N. C. *Adv. Organomet. Chem.* **1990**, *31*, 91. (e) Whitmire, K. H. Clusters of Metals and Nonmetals. In *Rings, Clusters and Polymers of Main Group and Transition Elements*; Roesky, H. W., Ed.; Elsevier, New York, 1989; pp 503−541.
(2) Lesch, D. A.; Rauchfuss, T. B. *Organometallics* **1982**, *1*, 506.
(3) Whitmire, K. H.; Shieh, M.; Lagrone, C. B.; Robinson, B. H.; Churchill, M. R.; Fettinger, J. C.; See, R. F. *Inorg. Chem.* **1987**, *26*, 2798.
(4) (a) Sigwarth, B.; Zsolnai, L.; Berke, H.; Huttner, G. *J. Organomet. Chem.* **1982**, *226*, C5. (b) Huttner, G.; Weber, U.; Sigwarth, B.; Scheidsteger, O. *Angew. Chem.* **1982**, *94*, 210; *Angew. Chem., Int. Ed. Engl.* **1982**, *21*, 215. (c) Huttner, G.; Weber, U.; Zsolnai, L. *Z. Naturforsch. B* **1982**, *37*, 707.
(5) Doedens, R. J. *Inorg. Chem.* **1969**, *8*, 570.
(6) Clegg, W.; Sheldrick, G. M.; Stalke, D.; Bhaduri, S.; Khwaja, H. K. *Acta Crystallogr.* **1984,** *C40*, 2045.
(7) Bautista, M. T.; Jordan, M. R.; White, P. S.; Schauer, C. K. *Inorg. Chem.* **1993**, *32*, 5429.
(8) Cook, S. L.; Evans, J.; Gray, L. R.; Webster, M. *J. Organomet. Chem.* **1982**, *236*, 367.
(9) Bartlett, R. A.; Rasika Dias, H. V.; Flynn, K. M.; Olmstead, M. M.; Power, P. P. *J. Am. Chem. Soc.* **1987**, *109*, 5699.
(10) Bautista, M. T.; White, P. S.; Schauer, C. K. *J. Am. Chem. Soc.* **1991**, *113*, 8963.
(11) Koide, Y.; Bautista, M. T.; White, P. S.; Schauer, C. K. *Inorg. Chem.* **1992**, *31*, 3690.
(12) Huttner, G.; Mohr, G.; Frank, A.; Schubert, U. *J. Organomet. Chem.* **1976**, *118*, C73.
(13) Gorzellik, M.; Nuber, B.; Ziegler, M. L. *J. Organomet. Chem.* **1992**, *436*, 207.
(14) Bachman, R. E.; Miller, S. K.; Whitmire, K. H. *Organometallics* **1995**, *14*, 796.
(15) Whitmire, K. H.; Leigh, J. S.; Luo, S.; Shieh, M.; Fabiano, M. D.; Rheingold, A. L. *New J. Chem.* **1988**, *12*, 397.
(16) This work.
(17) Whitmire, K. H.; Raghuveer, K. S.; Churchill, M. R.; Fettinger, J. C.; See, R. F. *J. Am. Chem. Soc.* **1986**, *108*, 2778.
(18) (a) Wei, C. H.; Dahl, L. F. *Inorg. Chem.* **1965**, *4*, 493. (b) Bard, A. J.; Cowley, A. H.; Leland, J. K.; Thomas, G. J. N.; Norman, N. C.; Jutzi, P.; Morley, C. P.; Schlüter, E. *J. Chem. Soc., Dalton Trans.* **1985**, 1303.
(19) Dahl, L. F.; Sutton, P. W. *Inorg. Chem.* **1963**, *2*, 1067.
(20) Schumann, H.; Magerstädt, M.; Pickardt, J. *J. Organomet. Chem.* **1982**, *240*, 407.

S0020-1669(96)00243-1 CCC: $14.00

Table 1. Structural Data for Selected Compounds Having an $E_2Fe_3(CO)_9$ Core Geometry

compound	<M−E−M	E···E	<E···E−R	ref
$Fe_3(CO)_9S_2$ (**1**)	98.4	2.86		18
$Fe_3(CO)_9Se_2$ (**2**)	96.6 (av)	3.10		19
$Fe_3(CO)_9Te_2$ (**3**)	96.5 (av)	3.36		20
$[Fe_3(CO)_9\{\mu_3\text{-}AsFe(CO)_4\}_2]^{2-}$ (**4**)	101.7	2.95	173.2	14
	102.5		173.2	
$[Fe_3(CO)_9\{\mu_3\text{-}SbFe(CO)_4\}_2]^{2-}$ (**5**)	101.2	3.20	174.2	15
	100.5		174.1	
$[Fe_3(CO)_9Bi_2]^{2-}$ (**6**)	96.8	3.54		16
	96.9			
$[Fe_3(CO)_9Bi(\mu_3\text{-}BiFe(CO)_4)]^{2-}$ (**7**)	101.9 (Fe)	3.40	173.4	17
	97.4			
$Fe_3(CO)_9(NMe)_2$	104.7	2.24	175.1	5
$Fe_3(CO)_9(NPh)_2$	103.3	2.30	173.8	6
	104.0			
$Fe_3(CO)_9(PH)_2$	107.6	2.58	179.1	7
	106.7		178.2	
$Fe_3(CO)_9(PPh)_2$	106.8	2.59		8
	107.0			
	106.3			
	106.9			
$Fe_3(CO)_9(P\text{-mesityl})_2$	106.1	2.65	174.9	9
$Fe_3(CO)_9\{PFe(CO)_2Cp\}_2$	103.2	2.73	171.2	10
	104.5		173.4	
$Fe_3(CO)_9\{PFe(CO)_2(C_5H_4Me)\}_2$				
molecule 1	103.1	2.74	171.4	10
	104.8		177.4	
molecule 2	104.4	2.71	171.4	
	106.2		176.7	
$[PPN]_2[Fe_3(CO)_9\{PMn(CO)_2Cp\}_2]$	103.5	2.77	171.0	11
	102.4		171.9	
$Fe_3(CO)_9\{AsPh\}_2$	105.3	2.79	174.3	12
	105.7		175.7	
$Fe_3(CO)_9\{AsMo(CO)_3Cp\}_2$	101.9	2.96	174.2	13
	101.8		173.8	

bond angles lower than the ideal 109.47° value.[21] Additionally, the value of α might be influenced by the strength of a possible E···E through-space interaction, as suggested by the short E···E nonbonding contacts which are present in all of these clusters.

Questions then arise as to the nature of these E−E interactions. Are they short nonbonding contacts resulting from some cage strain within the distorted square-pyramidal E_2M_3 framework (and what would be the electronic origin of this strain)? Do they arise from direct bonding interactions related to the tendency of the E atoms to reach hypervalency, as shown by the previous MO analysis on the related compounds $[E_2Co_4(CO)_{10}(\mu\text{-}CO)]^{1-/2-}$ (E = Sb, Bi)[22] and $[Fe_2(CO)_6Bi_2\{Co(CO)_4\}]^-$?[23] Can other factors explain the shortening of the E−E vector? Over the past several years, a body of data has accumulated on structures with cores of the type $Fe_3(CO)_9E_2$, $Fe_3(CO)_9(E)(ER)$, and $Fe_3(CO)_9(ER)_2$ which have prompted us to investigate these questions by extended Hückel molecular orbital calculations, which are reported here. This paper also describes the synthesis and structure of $[NEt_4]_2[Fe_3(CO)_9Bi_2]$, which we had reported earlier from the reduction of $Bi_2Fe_3(CO)_9$ but which had eluded structural characterization due to its instability in some solvents.[3]

Experimental Section

General Considerations. All reactions were performed under an inert atmosphere of nitrogen or argon using standard Schlenk/vacuum line techniques. Diethyl ether and tetrahydrofuran (THF) were dried by distillation from CaH_2 followed by distillation from Na/Ph_2CO ketyl. Acetonitrile was distilled from CaH_2 prior to use. Infrared spectra were obtained with a Perkin-Elmer Model 1640 FTIR instrument, and ^1H (250.13 MHz) and $^{13}C\{1H\}$ (62.90 MHz) NMR spectra were measured on a Bruker AC 250 spectrometer in the solvent noted. Analyses for carbon monoxide content were performed by digestion of the compound with $[PyH]Br_3$ in degassed CH_2Cl_2 at 75 °C in a vacuum flask, followed by quantitation of the liberated CO using a Toepler pump. The starting materials, $Fe_3(CO)_9Bi_2$[24] and $[NEt_4]_2[Bi_4Fe_4(CO)_{13}]$,[25] were prepared by literature methods. KC_8 was prepared by slow addition of potassium metal to stirred graphite flakes at 190 °C under argon.

Synthesis of $[NEt_4]_2[Fe_3(CO)_9Bi_2]$ (6). Method 1. Approximately 50 mL of MeCN was added to a 100 mL Schlenk flask containing $Fe_3(CO)_9Bi_2$ (0.272 g, 0.325 mmol) and KC_8 (2 equiv, 0.088 g, 0.649 mmol). The reaction was stirred for 30 min under argon. $[NEt_4]Br$ (2 equiv, 0.649 mmol, 0.136 g) was added, and the mixture stirred for an additional 15 min. The solution was then filtered through diatomaceous earth, and the solvent was removed from the deep brown solution in vacuo. The solid was extracted into THF, filtered, and the solvent was again removed under vacuum. The dark brown product was washed with Et_2O and dried under vacuum to give $[NEt_4]_2[Fe_3(CO)_9Bi_2]$. Yield: 0.125 g, 35% (based on Bi or Fe).

Method 2. MeCN (100 mL) was added to a 250 mL Schlenk flask containing $[NEt_4]_2[Bi_4Fe_4(CO)_{13}]$ (0.423 g, 0.251 mmol). The solution was heated at reflux for 6 h under argon and was then filtered through diatomaceous earth. The solvent was removed in vacuo and the solid washed with Et_2O and dried under vacuum to give pure **6**. Yield: 0.269 g, 74% (based on Fe). The compound may be crystallized by vapor-phase diffusion of Et_2O into a concentrated solution of **6** in MeCN. IR (ν_{CO} in cm^{-1}, MeCN): 1923 (vs), 1903 (ms), 1874 (m). ^1H NMR (CD_3CN): δ 3.17 (q, CH_2), 1.21 ppm (tt, CH_3). $^{13}C\{1H\}$ NMR (CD_3CN, 0.5 wt % $Cr[MeCOCH{=}C(O)Me]_3$, 293K): δ 222.9 (s, CO), 221.1 (s, CO), 219.7 (s, CO), 217.9 (s, CO), 53.6 (t (1:1:1), CH_3), 8.2

(21) (a) Gillespie, R. J.; Nyholm, R. S. *Q. Rev. Chem. Soc.* **1957**, *11*, 339. (b) Searcy, A. W. *J. Chem. Phys.* **1958**, *28*, 1237. (c) Searcy, A. W. *J. Chem. Phys.* **1959**, *31*, 1. (d) Gillespie, R. J. *J. Am. Chem. Soc.* **1960**, *82*, 5978. (e) Gillespie, R. J. *J. Chem. Educ.* **1963**, *40*, 295. (f) Gillespie, R. J. *J. Chem. Educ.* **1970**, *47*, 18. (g) Gillespie, R. J. In *Molecular Geometry*, Van Nostrand-Reinhold: London, 1972.

(22) Albright, T. A.; Ae Yee, K.; Saillard, J.-Y.; Kahlal, S.; Halet, J.-F.; Leight, J. S.; Whitmire, K. H. *Inorg. Chem.* **1991**, *30*, 1179.

(23) Kahlal, S.; Halet, J.-F.; Saillard, J.-Y.; Whitmire, K. H. *J. Organomet. Chem.* **1994**, *478*, 1.

(24) Churchill, M. R.; Fettinger, J. C.; Whitmire, K. H. *J. Organomet. Chem.* **1985**, *284*, 13.

(25) Whitmire, K. H.; Albright, T. A.; Kang, S.-K.; Churchill, M. R.; Fettinger, J. C. *Inorg. Chem.* **1986**, *25*, 2799.

Table 2. Crystal Data and Structure Refinement for $[Et_4N]_2[Bi_2Fe_3(CO)_9]$

empirical formula	$C_{25}H_{40}Bi_2Fe_3N_2O_9$
formula weight	1098.10
temperature	223(2) K
wavelength	0.7107 Å
crystal system	orthorhombic
space group	$P2_12_12_1$ (No. 19)
unit cell dimensions	
a	7.2800(10) Å
b	20.642(4) Å
c	22.365(4) Å
U	3360.9(10) Å^3
Z	4
ρ_{calc} (g/cm^3)	2.170
μ (mm^{-1})	11.749
F(000)	2080
crystal size	0.2 × 0.4 × 0.5 mm
θ range for data collection	2.07−27.49°
index ranges	$-7\le h\le 9$, $-22\le k\le 24$, $-21\le l\le 29$
no. of reflections collected	6228
no. of independent reflections	5619 [*R*(int) = 0.0697]
refinement method	full-matrix least-squares on F^2
data/restraints/parameters	5612/26/374
goodness-of-fit on F^2	1.012
final *R* indices [$I > 2\sigma(I)$]	$R_1 = 0.0680$, $_wR_2 = 0.1744$
R indices (all data)	$R_1 = 0.1222$, $_wR_2 = 0.2205$
F_{abs} [ext coeff]	0.68(2), [0.0004(2)]
largest diff peak and hole	1.696, −1.569 e/Å^3

ppm (br, CH_2). Anal. Calcd: CO, 0.84 mmol. Found: CO, 0.82 mmol. **6** is soluble in MeCN, THF, and Me_2CO, slightly soluble in CH_2Cl_2, but insoluble in Et_2O and hexanes.

X-ray Structure Determination of 6. A summary of data collection parameters for **6** is found in Table 2. The data were measured using a Rigaku AFC5S four-circle automated diffractometer (Rigaku CONTROL Automatic Data Collection Series, Molecular Structure Corp., The Woodlands, TX) using graphite-monochromated Mo Kα radiation (0.7107 Å). The crystal was mounted on a glass fiber with Epoxy cement, and data were collected with $2\theta z-\omega$ scans at 4°/min. Three standard reflections were monitored for decay every 150 reflections throughout data collection. An absorption correction from azimuthal (ψ) scans was applied to the data. The programs used in solving the structure were part of the Siemens Analytical X-Ray Instruments data reduction and refinement package SHELXTL PC,[26] and refinement of the structure was performed using the data refinement program package SHELXL-93.[27] A refinement weighting scheme of $w^{-1} = [\sigma^2(F_o^2) + (aP^2) + bP]$ was used, where the term $P = [(F_o^2) + 2(F_c^2)]/3$. Final residuals were calculated as $R_1 = \sum||F_o| - |F_c||/\sum|F_o|$ for $F_o^2 > 2\sigma(F_o^2)|$ and $_wR_2 = \{\sum[w(F_o^2 - F_c^2)^2]/\sum[wF_o^4]\}^{1/2}$ for all data, and the goodness of fit was calculated based on F^2 for all data.

Large dark crystals of **6** were obtained by the procedure described above. A tabular crystal (0.2 × 0.4 × 0.5 mm^3) was used for data collection, with the primitive unit cell determined from 25 random reflections and shown to be orthorhombic. The chiral space group $P2_12_12_1$ (No. 19) was chosen on the basis of reflection intensity statistics. During refinement the Flack parameter indicated that a mixture of the two enantiomeric forms was present in the crystal, which upon refinement gave a ratio of 2:1 for the two forms. The structure was solved by direct methods using the program XS, part of the SHELXTL-PC package, to locate the Bi and Fe atoms, and subsequent least-squares difference maps and Fourier syntheses using SHELXL-93 to find the remaining non-hydrogen atoms. The hydrogen atom positions of the counterion were calculated using the HFIX routine and were treated via a riding model tied to the carbon atom to which they are associated. All non-hydrogen atoms were refined anisotropically. The data were corrected for absorption (ψ scans) and a secondary extinction coefficient was calculated. Decay was insignificant, so no correction for this was made. The largest peak in the final difference map was 1.696 e/Å^3 and is a shadow peak off of bismuth.

(26) SHELXTL-PC, crystal structure solution and refinement package, Siemens Analytical X-Ray Instruments, Inc., Monterey, CA, 1990.
(27) Sheldrick, G. M. SHELXL-93, crystal structure refinement program, University of Göttingen, Göttingen, Germany, 1993.

Computational Details. Calculations have been carried out within the standard extended Hückel formalism[28] using the modified Wolfsberg−Helmholz formula.[29] Standard atomic parameters were taken for H, C, and O.[30] Parameters for S,[31] Bi,[23] and Fe[32] were taken from the literature. It has been confirmed that a reasonable variation of these parameters does not modify significantly the qualitative conclusions of this study. The models considered in the calculations are $Fe_3(CO)_9S_2$, $[Fe_3(CO)_9(SH)_2]^{2+}$, $[Fe_3(CO)_9Bi_2]^{2-}$, $[Fe_3(CO)_9(BiH)_2]$, and $[Fe_3(CO)_9\{BiFe(CO)_4\}_2]^{2-}$. Idealized geometries of C_s symmetry were assumed, which would be an exact C_{2v} symmetry if not considering the CO ligands on the apical iron atom. The assumed bond distances were taken from averaged experimental values of related clusters.[16−18,24,25,33−35] These bond distances (Å) follow. (i) For the sulfur species: Fe−Fe = 2.59; Fe_{ap}−S = 2.25; Fe_{bas}−S = 2.23; Fe−C = 1.75; C−O = 1.15; S−H = 1.33. (ii) For the bismuth species: Fe−Fe = 2.80; Fe_{ap}−Bi = 2.64; Fe_{bas}−Bi = 2.67; Fe−C = 1.75; C−O = 1.15; Bi−H = 1.80; Bi−$Fe(CO)_4$ = 2.67. The OC−Fe−CO bond angles were all set to 90° for the cluster Fe atoms. Ideal values of 120 and 90° were assumed for the external $Fe(CO)_4$ substituents. Because it is generally not feasible to optimize bond distances within the EHMO method, the optimization of the angle α was carried out by assuming that all the bond distances remain constant, as routinely done for EHMO angular optimization. However, it has been confirmed that small variations of the cluster core bond lengths do not significantly change the results. In the case of the clusters bearing substituents on E [R = H or Fe$(CO)_4$] the E···E−R angles were also optimized concomitantly with α.

Results and Discussion

Structure of $[NEt_4]_2[Fe_3(CO)_9(\mu_3\text{-}Bi)_2]$ (6). Although **6** had been observed previously by reduction of $Bi_2Fe_3(CO)_9$ with $[Cp_2Co]$,[3] until now it had not been structurally characterized owing to its instability in some solvents such as THF and CH_2Cl_2. The compound is, however, apparently very stable in MeCN solution. The data we have obtained for this compound are illuminating in terms of the present theoretical studies, for it provides with $[Fe_3(CO)_9Bi(\mu_3\text{-}BiFe(CO)_4]^{2-}$ (**7**), the first pair of E_2M_3 square-pyramidal clusters for which both a ligated and unligated form have been structurally characterized. This allows a comparison of the structural parameters of the two E_2M_3 compounds containing the same elements and core structures but differing only in that one possesses a terminal iron carbonyl fragment attached to one of the bismuth atoms, allowing a more precise look at the effect of this ligand on the core structure of the molecule.

The X-ray crystal structure of **6** shows that the anion packs as discrete units in the crystal lattice with no short intermolecular interactions. There are two crystallographically unique $[NEt_4]^+$ cations per anion in the lattice, giving an overall ratio of two

(28) (a) Hoffmann, R. *J. Chem. Phys.* **1963,** *39*, 1397. (b) Hoffmann, R.; Lipscomb, W. N. *J. Chem. Phys.* **1962**, *36*, 2179.
(29) Ammeter, J. H.; Bürgi, H.-B.; Thibeault, J. C.; Hoffmann, R. *J. Am. Chem. Soc.* **1978**, *100*, 3686.
(30) Hinze, J.; Jaffé, H. H. *J. Chem. Phys.* **1963**, *67*, 1501.
(31) Hoffman, D.; Hoffmann, R.; Fisel, C. R. *J. Am. Chem. Soc.* **1982**, *104*, 3858.
(32) Albright, T. A.; Burdett, J. K.; Whangbo, M.-H. *Orbital Interactions in Chemistry*; John Wiley and Sons: New York, 1985.
(33) Churchill, M. R.; Fettinger, J. C.; Whitmire, K. H.; Lagrone, C. B. *J. Organomet. Chem.* **1986**, *303*, 99.
(34) Cassidy, J. M.; Whitmire, K. H. *Inorg. Chem.* **1991**, *30*, 2788.
(35) (a) Whitmire, K. H.; Lagrone, C. B.; Rheingold, A. L. *Inorg. Chem.* **1986**, *25*, 2472. (b) Whitmire, K. H.; Lagrone, C. B.; Churchill, M. R.; Fettinger, J. C.; Biondi, L. V. *Inorg. Chem.* **1984**, *23*, 4227. (c) Holliday, R. L.; Roof, L. C.; Hargus, B.; Smith, D. M.; Wood, P. T.; Pennington, W. T.; Kolis, J. W. *Inorg. Chem.* **1995**, *34*, 4392. (d) Lilley, G. L.; Sinn, E.; Averill, B. A. *Inorg. Chem.* **1986**, *25*, 1075. (e) Adams, R. D.; Babin, J. E.; Estrada, J.; Wang, J.-G.; Hall, M. B.; Low, A. A. *Polyhedron* **1989**, *8*, 1885. (f) Nelson, L. L.; Lo, F. Y.-K.; Rae, A. D.; Dahl, L. F. *J. Organomet. Chem.* **1982**, *225*, 309. (g) Wei, C. H.; Dahl, L. F. *Inorg. Chem.* **1965**, *4*, 1. (h) Markó, L.; Madach, T.; Vahrenkamp, H. *J. Organomet. Chem.* **1980**, *190*, C67.

Table 3. Selected Atomic Coordinates ($\times 10^4$) and Equivalent Isotropic Displacement Parameters ($Å^2 \times 10^3$) for **6**[a]

	x	*y*	*z*	*U*(eq)
Bi(1)	7624(1)	3703(1)	7999(1)	42(1)
Bi(2)	2977(1)	3350(1)	7669(1)	39(1)
Fe(1)	6043(5)	3175(2)	7036(2)	37(1)
Fe(2)	4560(6)	3866(2)	8629(2)	40(1)
Fe(3)	5001(5)	4388(2)	7476(2)	35(1)
C(11)	6511(40)	2450(14)	7427(12)	49(7)
C(12)	8071(44)	3337(13)	6631(12)	51(8)
C(13)	4627(47)	2921(12)	6413(12)	45(7)
C(21)	4850(61)	3114(13)	8963(12)	67(11)
C(22)	2264(40)	4066(14)	8889(10)	46(7)
C(23)	5737(36)	4430(14)	9065(11)	39(6)
C(31)	5160(39)	4452(11)	6702(11)	37(6)
C(32)	6533(44)	5008(16)	7709(14)	56(8)
C(33)	2982(31)	4810(13)	7574(11)	39(6)
O(11)	6863(31)	1954(9)	7644(9)	60(5)
O(12)	9362(34)	3398(11)	6341(10)	70(7)
O(13)	3876(40)	2693(10)	6021(10)	73(7)
O(21)	5113(38)	2623(11)	9206(10)	70(7)
O(22)	951(29)	4214(11)	9103(10)	59(6)
O(23)	6522(38)	4805(11)	9386(11)	77(7)
O(31)	5225(38)	4584(12)	6189(9)	71(7)
O(32)	7482(28)	5437(9)	7846(11)	68(6)
O(33)	1637(29)	5119(11)	7622(11)	69(6)

[a] *U*(eq) is defined as one third of the trace of the orthogonalized $\mathbf{U}_{ij}$ tensor.

Table 4. Selected Bond Distances (Å) and Angles (deg) for **6**

Bi(1)−Bi(2)	3.5380(14)	Bi(2)−Fe(2)	2.660(4)
Bi(1)−Fe(1)	2.675(4)	Bi(2)−Fe(3)	2.634(4)
Bi(1)−Fe(2)	2.660(4)	Fe(1)−Fe(3)	2.795(5)
Bi(1)−Fe(3)	2.647(4)	Fe(2)−Fe(3)	2.814(5)
Bi(2)−Fe(1)	2.668(4)		
Fe(1)−Bi(1)−Fe(2)	96.77(12)	Fe(1)−Bi(2)−Fe(2)	96.93(12)
Fe(1)−Bi(1)−Fe(3)	63.35(11)	Fe(1)−Bi(2)−Fe(3)	63.61(11)
Fe(2)−Bi(1)−Fe(3)	64.03(11)	Fe(2)−Bi(2)−Fe(3)	64.21(11)
Fe(1)−Bi(1)−Bi(2)	48.46(8)	Fe(1)−Bi(2)−Bi(1)	48.61(8)
Fe(2)−Bi(1)−Bi(2)	48.32(8)	Fe(2)−Bi(2)−Bi(1)	48.32(9)
Fe(3)−Bi(1)−Bi(2)	47.79(8)	Fe(3)−Bi(2)−Bi(1)	48.10(8)
Bi(1)−Fe(1)−Bi(2)	82.94(10)	Bi(1)−Fe(3)−Bi(2)	84.11(10)
Bi(1)−Fe(1)−Fe(3)	57.85(10)	Bi(1)−Fe(3)−Fe(1)	58.80(11)
Bi(2)−Fe(1)−Fe(3)	57.61(10)	Bi(1)−Fe(3)−Fe(2)	58.20(11)
Bi(1)−Fe(2)−Bi(2)	83.36(11)	Bi(2)−Fe(3)−Fe(1)	58.78(11)
Bi(1)−Fe(2)−Fe(3)	57.76(11)	Bi(2)−Fe(3)−Fe(2)	58.34(11)
Bi(2)−Fe(2)−Fe(3)	57.45(11)	Fe(1)−Fe(3)−Fe(2)	90.65(14)

cations per anion. The structure consists of a square pyramid with two bismuth and two iron atoms forming the basal array and a third iron atom in the apical position. Crystallographic data collection parameters, selected atomic coordinates, and selected bond distances and angles for compound **6** are given in Tables 2−4. A thermal ellipsoid plot showing the anion with the atom labeling scheme is given in Figure 1.

Unlike most of the square-pyramidal clusters studied here, which show a "puckering" distortion of the cluster basal plane toward a trigonal-bipyramidal geometry, the basal Bi_2Fe_2 plane of **6** is almost perfectly flat as in **7** (Figure 1). It appears that the size of bismuth relative to iron is well suited to the geometry of the molecule. The angles in the basal plane of the cluster (Fe−Bi−Fe, 96.85° av; Bi−Fe−Bi, 83.15° av) deviate significantly from 90°. The Fe−Bi−Fe angle is of primary interest for this paper. In **7**, the Fe−Bi−Fe angle for the bare bismuth atom is 97.38(5)°, very similar to this angle in **6**; however, the angle for the substituted bismuth atom [101.91(5)°] is significantly higher, and this trend is observed in all of these E_2M_3 clusters. The underlying causes of this difference will be discussed below.

The Bi−Bi separation [3.5380(14) Å] in **6** is formally nonbonding, but some interaction between the two centers may

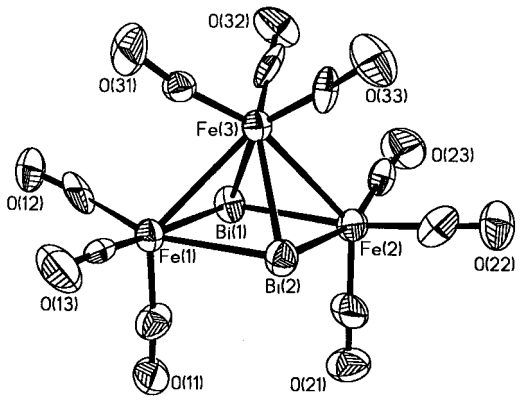

Figure 1. Thermal ellipsoid plot of **6** at 50% probability level with the atom labeling scheme. Carbon atom labels in the carbonyl ligands are omitted for clarity.

be present. The bismuth−iron distances, although somewhat shorter to the apical iron atom than to the atoms in the basal plane, are well within the normal bonding ranges observed in other Bi−Fe clusters[24,25] and complexes[33,34] and very close to those in **7**. The Fe(1,2)−Fe(3) distances (2.805 Å av) are considerably longer than the corresponding Bi−Fe distances (2.641 Å av) but are similar to those in **7** and in $Bi_2Fe_3(CO)_9$.[24] The C−Fe−C angles are as expected given the geometry of the molecule; however, the C−Fe−C angles around the apical iron Fe(3) are significantly larger than 90°, and the carbonyl ligands are tilted toward the cluster core. This is a commonly observed effect, and involves backbonding interactions from the M−E σ bonds into the π*-CO molecular orbitals.[36]

Calculations on E_2M_3 Clusters. (1) Sulfur Clusters. The α value optimized for the idealized $Fe_3(CO)_9S_2$ model is unrealistically too large and comes close to the one corresponding to the $[Fe_3(CO)_9(SH)_2]^{2+}$ model (∼105−107°). This is due to the geometry restrictions of the model which induces steric repulsions between the CO ligands attached to the basal iron atoms. Within the geometrical constraints of our models, this steric hindrance tends to repel the basal iron atoms and consequently tends to bring the sulfur atoms closer by increasing α. In the real molecule, this repulsion is minimized by some readjustment of the OC−Fe−CO bond angles.[18] We have circumvented the tedious cooptimization of several bond angles by artificially setting all the overlap integrals involved in these steric repulsions equal to zero. Under these conditions, the optimized α values are equal to 100 and 105° for $Fe_3(CO)_9S_2$ and $[Fe_3(CO)_9(SH)_2]^{2+}$, respectively. The first value is larger by ∼2° than the reported experimental ones.[18a] Considering the geometrical restrictions and the level of theory considered, this is a very satisfying agreement. The 5° increase of α when going from the sulfido cluster to the thiolato cluster is also in agreement with the trend observed between species in which E is a bare atom and compounds where E is substituted (see above and Table 1). A detailed analysis of the results indicates that, as intuitively expected, the 3s atomic orbital (AO) on sulfur is more involved in the bonding with the three iron atoms in $[Fe_3(CO)_9(SH)_2]^{2+}$ than in $Fe_3(CO)_9S_2$, whatever the value of α is. In other words, the presence of a substituent on S enhances the participation of 3s sulfur AO of $Fe_3(CO)_9S_2$ in the Fe−S

(36) (a) Alvarez, S.; Ferrer, M.; Reina, R.; Rossell, O.; Seco, M.; Solans, X. *J. Organomet. Chem.* **1989**, *377*, 291. (b) Silvestre, J.; Albright, T. A. *Isr. J. Chem.* **1983**, *23*, 139. (c) Graham, W. A. G. *Inorg. Chem.* **1968**, *7*, 315. (d) Lichtenberger, D. L.; Rai-Chaudhuri, A. *J. Am. Chem. Soc.* **1991**, *113*, 2923. (e) Parshall, G. W. *J. Am. Chem. Soc.* **1966**, *88*, 704. (f) Jetz, W.; Graham, W. A. G. *J. Am. Chem. Soc.* **1967**, *89*, 2773. (g) Willis, A. C.; van Buuren, G. N.; Pomeroy, R. K.; Einstein, F. W. B. *Inorg. Chem.* **1983**, *22*, 1162.

bonds. For example, at the abitrary value of $\alpha = 90°$, the $Fe_{bas}-S$ and $Fe_{ap}-S$ overlap populations in $Fe_3(CO)_9S_2$ are equal to 0.423 and 0.387, respectively, while for the same angle in $[Fe_3(CO)_9(SH)_2]^{2+}$ they are equal to 0.440 and 0.400, respectively.

It is clear then that the larger value computed for α in $[Fe_3(CO)_9(SH)_2]^{2+}$ results from the greater involvement of the sulfur 3s AOs in the Fe−S bonds. In fact, there is a complementary factor that favors a larger α angle in the case of the thiolato cluster: the S···S interaction. The experimental value for this nonbonding distance is consistent with a weak interaction (2.86 Å).[18a] This separation decreases as α increases. For example, in our models this distance varies from 3.15 to 2.56 Å as α changes from 90 to 110°. At $\alpha = 90°$, the computed S···S overlap population is slightly but significantly positive: 0.011 and 0.019 in the case of $Fe_3(CO)_9S_2$ and $[Fe_3(CO)_9(SH)_2]^{2+}$, respectively. When α increases, this overlap population curiously first decreases slightly before increasing again after 100°. This is due to a temporary bad orbital match in the range 95−100°. Nevertheless, whatever the S···S overlap population, it is always more attractive (or less repulsive) in the case of $[Fe_3(CO)_9(SH)_2]^{2+}$ than for $Fe_3(CO)_9S_2$. This effect also favors a larger angle α in the case of the substituted E ligand and originates in the depopulation of the σ^* (E···E) fragment orbital after interaction with the trinuclear $Fe_3(CO)_9$ fragment. It should be noted here that calculations on $Fe_3(CO)_9S_2$ using the Fenske−Hall approach have been reported previously.[37]

(2) Bismuth Clusters. In the case of the bismuth clusters, the square Fe_2E_2 base is flatter than in the sulfur models. As a consequence, the steric problems encountered in the sulfur species are absent for bismuth. The optimized α values for $[Fe_3(CO)_9Bi_2]^{2-}$, $[Fe_3(CO)_9(BiH)_2]$, and $[Fe_3(CO)_9\{BiFe(CO)_4\}_2]^{2-}$ are equal to 95, 101, and 100°, respectively. These values are in fairly good agreement with the experimental values reported in Table 1 for isoelectronic species having E as a heavy main group element. Again, the increase in α upon going from E (bare atom) to ER is nicely reproduced. In the case of $[Fe_3(CO)_9(BiH)_2]$ and $[Fe_3(CO)_9\{BiFe(CO)_4\}_2]^{2-}$, the Bi···Bi−R angle [R = H, $Fe(CO)_4$] is equal to 180 and 171°, respectively. The deviation from linearity in the case of R = $Fe(CO)_4$ corresponds to a bending "down" (i.e., away from the apical Fe atom) which compares well with those experimentally observed in **4** (173°),[14] **5** (174°),[15] and **7** (173°).[17] This slight bending is most likely steric in origin.

As with the sulfur species, the valence s AO of the Bi atom is more involved in the bonding when bearing a substituent, enhancing primarily the $Fe_{basal}-Bi$ bonds. For example, at the abitrary value of $\alpha = 100°$, the $Fe_{bas}-Bi$ and $Fe_{ap}-Bi$ overlap populations in $[Fe_3(CO)_9Bi_2]^{2-}$ are equal to 0.373 and 0.407, respectively, compared to 0.407 and 0.410 in $[Fe_3(CO)_9(BiH)_2]$ and to 0.390 and 0.394 in $[Fe_3(CO)_9\{BiFe(CO)_4\}_2]^{2-}$. The presence of substituents on Bi also affects the Bi···Bi overlap populations. Unlike the case of sulfur, the E···E overlap population is largely positive and increases monotonically as α increases. As expected, it is stronger in the case where E is a heavy main group element such as Bi, which bears more diffuse and high-lying atomic orbitals than sulfur. Also unlike the sulfur species, the Bi···Bi overlap population is smaller in the case of the substituted species. For example at $\alpha = 100°$, it is equal to 0.144, 0.076, and 0.106 for $[Fe_3(CO)_9Bi_2]^{2-}$, $[Fe_3(CO)_9(BiH)_2]$, and $[Fe_3(CO)_9\{BiFe(CO)_4\}_2]^{2-}$, respectively. This time, the E···E nonbonding interaction tends to favor larger α values for the unsubstitued species. From these results and those obtained with the sulfur clusters, we conclude that the existence of a weak bonding interaction is not the dominant factor in determining α upon going from clusters with bare E ligands to clusters with substituted E atoms.

Conclusions

Upon comparing the wide variety of main group transition metal carbonyl clusters containing a square-pyramidal E_2M_3 core, it was found that the M−E−M angles in the basal plane of the molecule are smaller when E is a bare atom than when it is substituted with a terminally appended ligand. Molecular orbital calculations using substituted and unsubstituted models in which the angles within the basal planes of these models were optimized reproduced the observed angular effect noted above, and it was found that, although the experimentally observed short nonbonding E···E interactions play a role in this effect, the primary influence on the angles in the E_2M_2 plane lies in the presence or absence of a lone pair of electrons on E. In the unsubstituted atoms, a lone pair resides in an AO of primarily s character; however, when a substituent exists on the main group atom, these electrons become more involved in bonding interactions and the M−E−M angle expands as the electrons become more localized.

Acknowledgment. The National Science Foundation (K.H.W.), the Robert A. Welch Foundation (K.H.W.), and the Centre Nationale de Recherche Scientifique (J.-Y.S.) are gratefully acknowledged for financial support of this work. The NSF and CNRS are also thanked for a joint travel grant to facilitate this collaboration.

Supporting Information Available: ORTEP plots with numbering schemes for the cations in the structure of **6** and full table of structural data on E_2M_3 clusters (23 pages). Ordering information is given on any current masthead page. An X-ray crystallographic file in CIF format for **6** is available on the Internet only. Access information is given on any current masthead page.

IC960243L

(37) Rives, A. B.; Xiao-Zeng, Y.; Fenske, R. F. *Inorg. Chem.* **1982**, *21*, 2286.